Academic Education Publishing House

*Industry Science and Engineering Vol. 2 No. 12, 2025*

# Research on the Spatiotemporal Evolution Characteristics and Prediction of Long-Term Ground Subsidence along Subway Lines based on SBAS-InSAR and RNN Models

**Xin Zhang[1], Yitong Wu[1], Zhaozhao Lu[2,*]**

[1]*China Jikan Research Institute of Engineering Investigations and Design Co., Ltd., Xi'an, Shaanxi, China*

[2]*Shannxi Nongfa Digital Intelligence Group, Xi'an, Shaanxi, China*

[*]*Corresponding Author*

**Abstract: Land subsidence has long threaened the safety of construction, operation and maintenance of urban rail transit, and subsidence along subway lines is directly critical to the full life-cycle safety of subway projects. To reveal the spatiotemporal evolution law of land subsidence along subway lines and achieve accurate prediction of subsidence trends, this study takes a subway line in Xi'an as a case. Using 67 Sentinel-1A images (2018.01–2025.03), we extracted long-term subsidence via SBAS-InSAR (validated by second-order leveling), analyzed its spatial distribution along subway line, and built an RNN model to predict subsidence at typical stations. Results show SBAS-InSAR agrees with leveling within ±3 mm (high reliability). Cumulative subsidence (2018–2025) ranges from 60 mm to −252.49 mm, with strong spatial heterogeneity along the Line and the most severe subsidence at Qujiang area. The RNN effectively captures diverse subsidence patterns and accurately predicts severe, stable, and decelerating trends, with predicted and observed evolutions highly consistent. This study provides data and technical support for construction optimization, operational hazard early warning, and subsidence control of Xi'an Subway Line and similar projects in Xi'an.**

**Keywords: SBAS-InSAR; Land Subsidence; Recurrent Neural Network (RNN); Subsidence Prediction**

## 1. Introduction

Land subsidence is one of the most common slow-onset and irreversible geological hazards affecting urban development [1,2]. Driven by both natural conditions and anthropogenic activities, it has become a critical geological issue restricting the high-quality advancement of urbanization. Obvious land subsidence has been observed in many regions of China, such as the North China Plain, Fenwei Basin, and Yangtze River Delta [3-5]. Among them, the Fenwei Basin where Xi'an is located features strong loess collapsibility and well-developed concealed faults, leading to a particularly prominent superimposed impact of land subsidence and ground fissure disasters. Such hazards not only disturb the planning and utilization of urban underground space and the construction of infrastructure, but also directly threaten the safe operation of lifeline projects including subways and underground pipelines, and even endanger people's lives and property in severe cases. Therefore, conducting long-term land subsidence monitoring along major subway projects, systematically analyzing its spatiotemporal evolution characteristics, and establishing accurate prediction models are of great practical significance for urban geological disaster prevention and engineering safety assurance.

Compared with traditional monitoring techniques such as Global Positioning System (GPS) and geometric leveling, Synthetic Aperture Radar Interferometry (InSAR) has been widely used in surface deformation monitoring, mining area deformation extraction, and seismic and volcanic activity research due to its advantages of all-day, all-weather and high-precision monitoring [6-11]. The Small Baseline Subset InSAR (SBAS-InSAR) technique was proposed by Berardino et al. in 2002 [12]. It forms interferometric pairs by reducing spatiotemporal baseline thresholds to overcome the spatiotemporal decorrelation in conventional InSAR algorithms, reduces the demand for SAR image quantity, improves solution efficiency,

and thus obtains high-precision deformation time series. At present, SBAS-InSAR has been extensively applied to deformation monitoring and disaster identification along subway lines. Deng et al. [13] monitored the areas along Urumqi Subway Lines 1 and 2 using SBAS-InSAR, and predicted subsidence trends with the autoregressive integrated moving average (ARIMA) model, identifying potential subsidence funnels along Subway Line 1. Yu et al. [14] investigated the evolutionary characteristics of surface subsidence along subway lines in downtown Hefei using InSAR, and explored the relationship between subsidence troughs and subways with the Peck model. Liu et al. [15] monitored and analyzed land subsidence along Beijing Subway Line 6 using InSAR, and deeply explored the subsidence inhomogeneity of typical sections based on the hierarchical entropy method. Qiao et al. [16] monitored subsidence along Nanjing subway lines using SBAS-InSAR, and analyzed its response to precipitation, finding that increased pore water pressure and gas pressure in soil affected subsidence. Han et al. [17] analyzed the inhomogeneous subsidence along subway lines in Futian District, Shenzhen using InSAR, improved the high-coherence point extraction algorithm to enhance monitoring accuracy, and discussed the correlation between subsidence and precipitation. Chen et al. [18] carried out long-term InSAR monitoring of land subsidence along subway lines in Fuzhou, detected eight subsidence funnels, and analyzed their formation mechanisms combined with geological conditions.

This Subway Line passes through concealed structural zones such as the Zaohe Fault and Chanhe Fault. The strata along the line are dominated by miscellaneous fill, loess-like soil, silty clay and medium sand interbeds, resulting in complex and variable geological conditions. Construction procedures including pilot tunnel excavation, support installation and grouting may disturb the stratal stress balance and induce ground subsidence of varying degrees. Meanwhile, the combined effect of regional groundwater level rebound and rainfall infiltration further elevates the risk of loess collapsible deformation, which may increase the complexity and uncertainty of the spatiotemporal distribution of subsidence along the line.

At present, most subsidence studies on Xi'an Subway Line are limited to local analyses of single stations or construction stages, lacking long-term dynamic monitoring covering the entire line from construction to the early operation period. Moreover, the understanding of subsidence evolution considering both geological background and engineering disturbance remains insufficient, which can hardly meet the safety management requirements for the full life cycle of the line.

Therefore, this study obtains long-term land subsidence monitoring data along the subway line from January 2018 to March 2025 based on SBAS-InSAR technology, and further analyzes the spatiotemporal evolution characteristics and prediction of land subsidence. The cumulative temporal variation and spatial distribution differences of subsidence along the line are interpreted, and the coupled influencing mechanism of subsidence is analyzed. A recurrent neural network (RNN) model is established to predict subsidence at typical sites. The results can provide data support for construction optimization and operational disaster early warning of Subway Line, and also offer a scientific reference for subsidence prevention and control of subway projects.

## 2. Data Set

The study area of this paper is shown in Figure 1. The SAR data source adopts Sentinel-1A synthetic aperture radar (SAR) images launched by the European Space Agency (ESA) in 2014. As part of a dual-satellite remote sensing system, the satellite is equipped with a C-band sensor capable of acquiring high-resolution surface observation data, with a range resolution of 5 m and an azimuth resolution of 20 m, respectively, and a revisit period of 12 days. In this experiment, 67 scenes of images covering the study area from January 2018 to March 2025 were selected for data processing via the SBAS-InSAR technique. The external Digital Elevation Model (DEM) data adopts the Shuttle Radar Topography Mission (SRTM) data provided by the National Aeronautics and Space Administration (NASA), with a spatial resolution of 90 m.

To verify the reliability of the subsidence monitoring results, geometric leveling data were used for validation in this study. A Trimble DiNi03 electronic level was adopted for leveling to arrange benchmark and monitoring points. Connected or closed leveling lines were designed for observation, and both the survey

grade and deformation measurement precision grade were set to the second order. The mean square error of height difference per monitoring point was controlled within 0.5 mm.

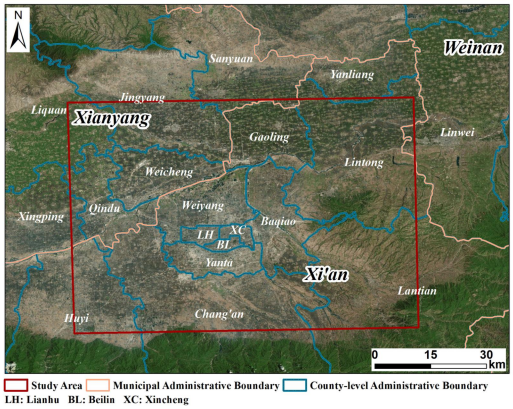


**Figure 1. The Study Area and Data Processing Scope**

## 3. Methods

### 3.1 SBAS-InSAR Technology

The core principle of SBAS-InSAR relies on multi-temporal SAR images over the same study area. Independent interferometric datasets are generated by forming interferometric pairs with spatiotemporal baselines constrained to predefined thresholds. Preprocessing steps including image coregistration, flat-Earth removal, filtering, and phase unwrapping are then applied to each pair, producing interferometric phase maps that contain surface deformation, topographic signals, and atmospheric delay errors. External DEM data are adopted to eliminate the topographic phase component. With the aid of atmospheric phase correction models (e.g., linear correction using meteorological data or spatiotemporal filtering), the atmospheric delay effect is separated and reduced. The cumulative deformation sequence and deformation rate field of the surface are finally inverted through time-series phase modeling. The flowchart of the SBAS-InSAR processing implemented in this study is illustrated in Figure 2, and the main procedures are as follows.

To meet the land subsidence monitoring requirements along the Subway Line, 67 scenes of Sentinel-1A images in Single Look Complex (SLC) format were imported and cropped in this study, so as to reduce spatial decorrelation and noise interference caused by mountainous areas (e.g., the Qinling Mountains) and vegetation cover around the city. All images were coregistered, and the full spatiotemporal baseline information was extracted. The thresholds were set as follows: minimum temporal baseline =120 days, maximum spatial baseline = 300m, and maximum allowable Doppler shift = 291.892. The interferometric phase consists of contributions from multiple phase components, including Earth curvature phase, topographic phase, noise phase, atmospheric delay phase, and surface deformation phase, as expressed in Equation (1) [19]. The topographic phase components in the azimuth and range directions induced by Earth curvature were removed by generating the topographic phase trend using the Earth ellipsoid and baseline model. After filtering with the Goldstein adaptive filter to reduce noise phase and residuals, 40 control points were selected in regions far from deformation zones, free of residual topographic phase and discontinuities, for three rounds of orbit refinement and re-flattening. Phase unwrapping was performed using the minimum cost flow (MCF) algorithm to improve the coherence of interferometric results. The unwrapping coherence threshold was set to 0.3, and the maximum buffer radius of ground control points for valid pixels in the slant-range geometry unwrapping results was 22.5 m.

$$\varphi = \varphi_{def} + \varphi_{topo} + \varphi_{orb} + \varphi_{atm} + \varphi_{noise} \quad (1)$$

$$\varphi_{def} = \frac{4\pi}{\lambda} d \quad (2)$$

Where $\varphi_{topo}$ is the residual topographic phase caused by DEM errors, $\varphi_{orb}$ is the orbital error phase, $\varphi_{def}$ is the line-of-sight (LOS) deformation phase, $\varphi_{atm}$ is the atmospheric delay phase related to the time interval, and $\varphi_{noise}$ represents other errors from coregistration and other processes. d denotes the LOS deformation displacement, and λ is the radar wavelength. Equation (2) describes the relationship between the LOS deformation component and the wavelength [20]. Finally, the time-series deformation model was solved using the Singular Value Decomposition (SVD) method to obtain the spatial distribution of cumulative subsidence and annual average subsidence rate over the study area, providing data support for the subsequent analysis of spatiotemporal evolution characteristics of land subsidence.

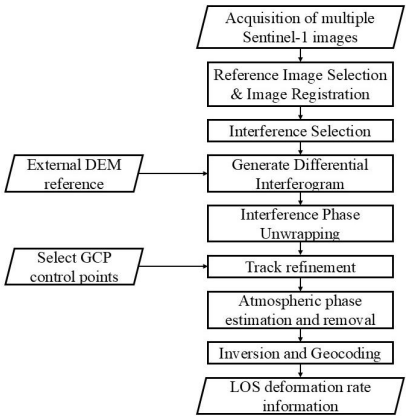


**Figure 2. SBAS-InSAR Technical Flowchart**

### 3.2 Recurrent Neural Network (RNN)

RNN is a class of artificial neural networks with internal cyclic connections, designed for processing sequential data. Its most prominent feature is the presence of loops within the network, which allows information to circulate and enables the storage and processing of sequential information. An RNN can accept an input sequence and transmit it to the hidden layer; cyclic connections exist between hidden layers, enabling the network to maintain a "memory" state that contains historical information. This allows RNNs to capture contextual information within sequences. RNNs can have one or more outputs—for instance, in sequence generation tasks, an output is produced at each time step. In this study, the monthly cumulative subsidence data of the study area from January 2018 to March 2025 obtained via SBAS-InSAR were used as the base time-series data. Subsidence sequences of typical subway stations along Subway Line were selected as the dataset for model training and validation. First, outliers were removed from the raw data, and then the dataset was divided into training, validation, and test sets in proportion: the training set was used for model parameter optimization, the validation set for preventing overfitting, and the test set for evaluating the final predictive performance of the model. The model adopted a three-layer structure of "input layer-hidden layer-output layer": The number of neurons in the input layer was set according to the length of the time series, with the subsidence values of the previous n months selected as input features (the optimal time step n=6 was determined via cross-validation in this study); The hidden layer consisted of 2 neuron layers, with the Sigmoid function selected as the activation function to enhance the model's nonlinear fitting capability; The output layer contained 1 neuron, corresponding to the predicted subsidence value for the next month, and a linear function was used as the activation function to ensure the rationality of the physical meaning of the output value. To comprehensively evaluate the prediction accuracy of the RNN model, Root Mean Squared Error (RMSE), Mean Absolute Error (MAE), and coefficient of determination ($R^2$) were selected as evaluation metrics, with their calculation equations as follows:

$$RMSE = \sqrt{\frac{1}{N}\sum_{i=1}^{N}\left(y_i - \hat{y}_i\right)^2} \tag{3}$$

$$R^2 = 1 - \frac{\sum_{i=1}^{N}\left(y_i - \hat{y}_i\right)^2}{\sum_{i=1}^{N}\left(y_i - \bar{y}\right)^2} \tag{4}$$

Where N is the number of samples; $y_i$ is the measured subsidence value of the i-th sample; $\hat{y}_i$ is the corresponding predicted value; $\bar{y}$ is the mean value of the measured subsidence.

## 4. Results and Analysis

### 4.1 Analysis of Long-term Spatiotemporal Characteristics of Land Subsidence

The spatial distribution of cumulative vertical settlement (mm) in the study area from 2018 to 2025 was processed using SBAS InSAR technology, as shown in Figure 3. Overall, the cumulative ground subsidence from 2018 to 2025 ranges from 60mm to -252.49mm and exhibits uneven spatial distribution characteristics. Through comparative analysis of historical data, it is found that the spatial distribution of ground subsidence during the research period is still related to the direction of ground fissures and faults in Xi'an, and the center of ground subsidence has shifted and the degree of ground subsidence has slowed down. The experimental results show that surface uplift mainly occurs in the western suburban areas, with a belt like distribution along the F3-F8 direction of the ground fissures. The maximum surface uplift of 60mm is located near the Dianzicheng area, as one of the historical largest ground subsidence centers, has shown significant surface rebound. The cumulative surface uplift is 56.93mm, and the area with rebound exceeding 40mm reaches 2.78km2. This indicates that the limited exploitation of

groundwater resources and the control of ground subsidence have achieved significant results. Ground subsidence is more severe in three areas: the Sanyao-Hangtiandadao, the Qinglong Temple-International Convention and Exhibition Center, and the vicinity of Yuhuazhai. The maximum ground subsidence of 252.49mm is located in the Qinglong Temple International Convention and Exhibition Center area, with an average annual subsidence rate of 62.98mm/a; the maximum ground subsidence rate near Yuhuazhai reached 31.52mm/a, and the maximum cumulative subsidence amount reached 107.6mm. The development of ground subsidence in the Sanyao-Hangtiandadao and Qinglong Temple International Convention and Exhibition Center areas may be affected by the Chang'an-Lintong fault, and the ground subsidence near Yuhuazhai may be related to the rapid development of urban construction in the region.

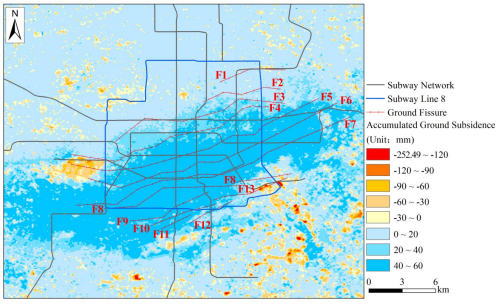


**Figure 3. SBAS-InSAR Technical Flowchart**

To further verify the accuracy of the land subsidence results derived from SBAS-InSAR processing, validation was conducted using 27 ground subsidence monitoring points in this experiment. The average subsidence of all coherent points within a 10-meter buffer centered at each monitoring point was taken as the InSAR monitoring value corresponding to the leveling point, and the difference between the two datasets was analyzed, as shown in Figure 4. The differences between geometric leveling measurements and InSAR monitoring values are all within ±3 mm. Existing literature [21] indicates that land subsidence in the Dianzicheng area has slowed annually after 2015 and even exhibited ground rebound in recent years, while subsidence in the Aerospace City zone along the Chang'an–Lintong Fault zone has continued to intensify. This is generally consistent with the spatial distribution and subsidence trends obtained in this study. It is comprehensively verified that the land subsidence results obtained by SBAS-InSAR are reliable.

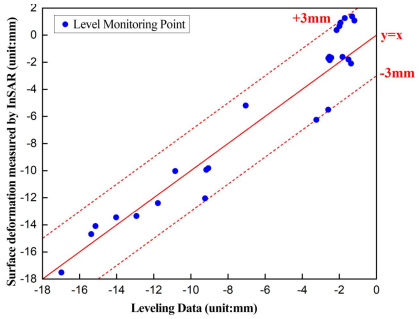


**Figure 4. Comparison between InSAR-Derived Land Subsidence Results and Leveling Measurements**

### 4.2 Analysis of Land Subsidence along the Subway Line

Based on the land subsidence results derived from SBAS-InSAR in the study area, a 300-meter radius buffer zone centered on this Subway Line was established to analyze the subsidence characteristics along the line, as presented in Figure 5. The results show that severe subsidence along Line is mainly distributed in three sections: P1–P3 (Figure 5b), P6–P7 (Figure 5c), and P8 (Figure 5d). The most serious subsidence occurs near P1, with a cumulative subsidence of 252.49 mm and an average annual subsidence rate of 62.98 mm/a. Subsidence in this area started early, developed rapidly, and reached a severe degree. The cumulative subsidence at P2 is 161.55 mm, with an average annual subsidence rate of 37.38 mm/a. The maximum cumulative subsidence near P6 is 66.11 mm, with an annual rate of 17.23 mm/a. For P7, the maximum cumulative subsidence is 57.26 mm, with an annual rate of 13.41 mm/a. Subsidence from P6 to P7 is relatively mild but covers a wide range. Near P8, the maximum subsidence is 80.39 mm, with an average annual rate of 16.14 mm/a, and the affected area is small. Subsidence in this region is likely influenced by the long-term subsidence funnel in the western suburbs.

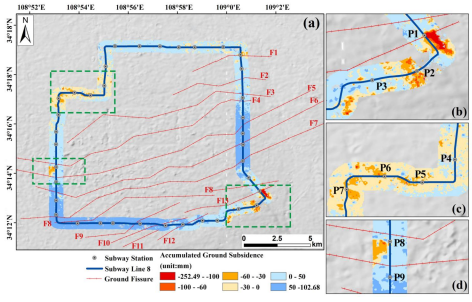


**Figure 5. Spatial Distribution of Cumulative Land Subsidence along Subway Line**

### 4.3 Subsidence Prediction for Major Subsiding Areas along the Subway Line

To further explore the evolutionary trend of land subsidence, a Recurrent Neural Network (RNN) model was adopted in this study to predict subsidence at the key subsiding subway stations shown in Figures 5b–5d. Monitoring data within a 300 m radius centered on each station were selected as samples, with the sample size ranging from 500 to 1000. The first 57 phases of subsidence data were used for model calculation, and the last 10 phases for model testing. The model parameters were set as follows: learning rate = 0.01, 4 hidden layer neurons, 1 output layer neuron, training epochs = 1000, and maximum allowable error = 0.00001. The results are displayed in Figure 6. In Figure 6, the black solid line represents the actual cumulative subsidence series obtained by InSAR, the blue dashed line represents the model-predicted values, the red dashed line separates the model training period (2018.01 –2025.03) and prediction period (2025.04 –2028.12), and the gray shaded area denotes the model prediction interval. The actual subsidence series reveal that land subsidence along the Subway Line exhibited strong spatial heterogeneity during 2018–2025, and the RNN model presents a good capability in capturing the subsidence trend of each station.

The prediction results show that: Subsidence at P1 displays a continuously intensifying trend. The predicted values are highly consistent with the measured values in the changing direction, with only a slight deviation in magnitude, reflecting the model's adaptability to intense subsidence processes. Predictions at P2 agree well with the steady subsidence characteristics in the later observation period, and the predicted series shows small fluctuations, indicating the model's good fitting ability for stable deformation trends. Predicted values at P8 fluctuate slightly within the gray interval, consistent with the gradual mitigation of actual subsidence in the later stage, and the model effectively captures the attenuation process of the subsidence rate. Predictions for P7 follow the downward trend of the observed subsidence. Although the predicted amplitude is slightly larger than the measured value, the trend direction is consistent, verifying the model's reliability in judging the subsidence evolution direction. Predictions for P6 reflect the phased characteristic of "fast first, then slow" in the actual subsidence process. The model successfully captures the variation in subsidence rate, which matches the real evolutionary law.

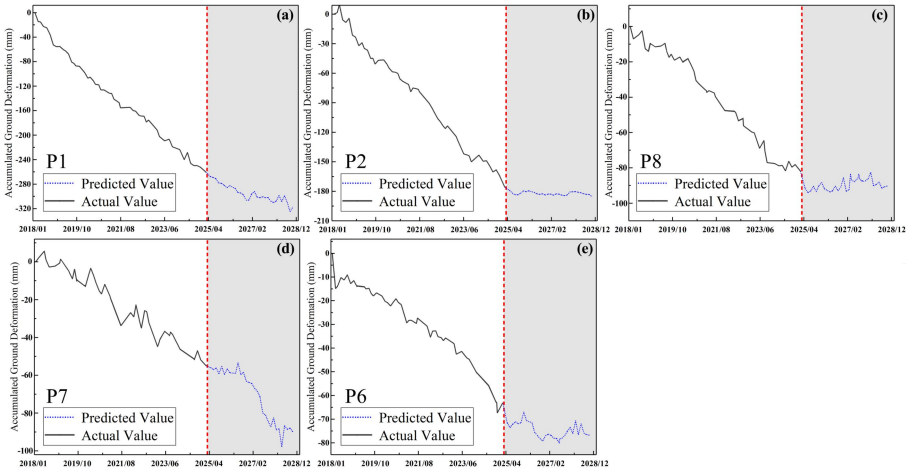


**Figure 6. Time-Series Prediction Results of Land Subsidence Using the RNN Model**

In general, the RNN model can effectively capture the spatiotemporal evolution of land subsidence at different stations along Subway Line, and achieves favorable prediction performance for subsidence trends with different magnitudes and rates. It can provide reliable technical support for long-term monitoring and risk early warning of land subsidence along subway lines.

## 5. Results and Discussion

Taking a Xi'an Subway Line as the research object, this study obtained long-term land subsidence monitoring data of the study area from January 2018 to March 2025 based on SBAS-InSAR technology, and completed leveling verification of the monitoring results. The spatiotemporal evolution characteristics of land subsidence in the study area and along Subway Line were systematically analyzed, and

an RNN model was constructed to predict the subsidence trend of typical subsiding stations. The main conclusions are as follows:

(1) SBAS-InSAR technology can effectively realize high-precision and long-term monitoring of land subsidence in Xi'an urban area and along Subway Line. Verified by second-order geometric leveling data, the differences between InSAR and leveling results are all controlled within ±3 mm, which proves the reliability of InSAR monitoring results.

(2) Land subsidence in the study area from 2018 to 2025 shows significant spatiotemporal heterogeneity, with cumulative subsidence ranging from 60 mm to −252.49 mm. The spatial distribution is highly correlated with the strikes of regional ground fissures and faults, the subsidence center has shifted, and the overall subsidence degree has been mitigated. Obvious ground rebound occurs in historical subsidence centers such as Dianzicheng, which confirms the remarkable effect of subsidence prevention and control measures including regional groundwater extraction restriction. Qinglongsi–International Convention and Exhibition Center, Sanyao–Hangtian Avenue, and Yuhuazhai are the three major subsidence areas in the study area, and subsidence development is jointly affected by concealed faults and urban engineering construction activities.

(3) Land subsidence along the Subway Line is concentrated in three sections: P1 to P2, P6 to P7, and P8, with obvious spatial differences in subsidence development. P1 is the most seriously subsided station along the line, with a cumulative subsidence of 252.49 mm, characterized by early occurrence and high subsidence rate. P8 shows local subsidence affected by western suburban settlement funnel. Subsidence from P6 to P7 is relatively mild but covers a wide range. The subsidence characteristics of each station are closely related to the regional geological background and engineering disturbance.

(4) The RNN model constructed based on the monthly cumulative subsidence monitored by InSAR has good prediction ability for the subsidence trend of 5 typical subsiding points along Subway Line. The model can accurately capture the continuous intense subsidence at P1 and the stable subsidence at P2 in the later period. It can also effectively identify the attenuation process of subsidence rate at P8 and the phased subsidence characteristic of "fast first, then slow" at P6. Although there are slight deviations in subsidence magnitude of predicted values at some stations, the overall evolution trend is highly consistent with the actual situation, which proves the applicability and effectiveness of the RNN model in land subsidence prediction along urban subway lines.

The spatiotemporal evolution law of land subsidence along the Subway Line and the subsidence prediction model constructed in this study can provide technical support for dynamic land subsidence monitoring and geological disaster risk early warning during the line operation period, and also provide a scientific basis for the formulation of subsequent subsidence prevention and control engineering measures. Subsequent research can further optimize the RNN model by combining multi-source data such as regional groundwater level change, stratigraphic lithology and engineering construction activities, so as to improve the accuracy and timeliness of subsidence prediction. Meanwhile, the coupling effect between subsidence and ground fissures along subway lines can be studied to provide more comprehensive theoretical and technical support for the full life cycle safety management of subway projects.

**Acknowledgments**

This paper is supported by the Shaanxi Provincial Innovation Capacity Support Program under the project entitled Intelligent Digital Detection and Monitoring Platform for the State of Urban Underground Engineering (Grant No. 2024CX-GXPT-17).

**References**

[1] Yin Y, Zhang Z, Zhang K. Land Subsidence and Countermeasures for its Prevention in China. The Chinese Journal of Geological Hazard and Control, 2005, (02):1-8.

[2] Wu J. Method and Application of Land Subsidence Disaster Regionalization, SHANGHAI LAND & RESOURCES. 2011, 32(02): 84-7.

[3] Ge D. Research on the Key Techniques of SAR Interferometry for Regional Land Subsidence Monitoring. China University of Geosciences (Beijing), 2013.

[4] Zhang S, Li M, Liu Z, et al. Temporal and Spatial Distribution Characteristics of Land Subsidence in Xi'an-Xianyang Interpreted by Time-Series InSAR. Journal of Geodesy

and Geodynamics. 2024, 44 (04):391-397.
[5] Li J, Zhang S, Sheng L, et al. Research on Ground Subsidence Monitoring in Xi'an using Time-series InSAR and Universal GNSS. Bulletin of Surveying and Mapping. 2026, (01):18-24+46.
[6] Ferretti A, Prati C, Rocca F. Permanent scatterers in SAR Interferometry. IEEE Transactions on Geoscience & Remote Sensing, 2001, 39(1):8-20.
[7] Gabriel A K, Goldstein R M, Zebker H A. Mapping Small Elevation Changes over Large Areas: Differential Radar Interferometry. Journal of Geophysical Research Solid Earth, 1989, 94(B7):9183-9191.
[8] Massonnet D, Feigl K L. Radar Interferometry and its Application to Changes in the Earth's Surface. Reviews of Geophysics, 1998.
[9] Qu F, Zhang Q, et al. Land Subsidence and Ground Fissures in Xi'an, China 2005–2012 Revealed by Multi-band InSAR Time-series Analysis. Remote Sensing of Environment, 2014, 155:366-376.
[10]Chen G, Shan X, Woolk M Moon, et al. A modeling of the magma chamber beneath the Changbai Mountains volcanic area constrained by InSAR and GPS derived deformation. Chinese Journal of Geophysics. 2008, (04): 1085-92.
[11]Wan Y, Shen Z, Wang M, et al. Coseismic Slip Distribution of the 2001 Kunlun Mountain Pass West Earthquake Constrained using GPS and InSAR data. Chinese Journal of Geophysics. 2008, (04): 1074-84.
[12]Berardino P, Fornaro G, Lanari R, et al. A New Algorithm for Surface Deformation Monitoring Based on Small Baseline Differential SAR Interferograms. IEEE Transactions on Geoscience & Remote Sensing, 2002, 40(11):2375-2383.
[13]Deng W, Deng L. Cao S. Application of SBAS-InSAR and ARIMA Models in Monitoring Subway Line Settlement: A Case Study of Urumqi. Urban Rapid Rail Transit, 2025, 38(6): 55-62.
[14]Yu S, Chen L. Yang Y, et al Application of InSAR technology in deformation monitoring of Hefei subway. Science of Surveying and Mapping, 2022, 47(3): 96-10, 109.
[15]Liu K S, Gong H L, Chen B B. Monitoring and Analysis of Land Subsidence of Beijing Subway Line 6 based on InSAR Data. Journal of Geo-information Science, 2018, 20(1):128-137.
[16]Qiao S, Sun C, Bi L et al. Analysis of Settlement Monitoring along the Subway Line in Nanjing based on Time Series InSAR Technology. Bulletin of Surveying and Mapping, 2024, (10):64-70.
[17]Han K, Leng L, Zhang J, et al. Spatio-temporal Analysis of Surface Subsidence along the Futian Subway Line based on Time-series InSAR Technology. Bulletin of Surveying and Mapping, 2025, (S2):89-93+179.
[18]Chen A, Tan Y, Yang C, et al. Deformation Monitoring along Fuzhou Subway Line based on Radar Technology. Surveying and Mapping Science. 2021(7): 86-91.
[19]Hooper A, Zebker H, Segall P et al. A new method for measuring deformation on volcanoes and other natural terrains using InSAR persistent scatterers. Geophysical Research Letters, 2004, 31(23).
[20]Shao Y, Ma J, Han L, et al. Time series analysis and prediction of surface subsidence based on SBAS-InSAR technology. Bulletin of Surveying and Mapping, 2025, (04):51-57+62.
[21]Zhao C, Zhang Q, Ding X, et al. InSAR Based Evaluation of Land Subsidence and Ground Fissure Evolution at Xi'an. Journal of Engineering Geology. 2009, 17(03): 389-93.